Electronic Supplementary Material (ESI) for Physical Chemistry Chemical Physics.

On-surface synthesis of extended linear graphyne molecular wires by protecting the alkynyl group

Francesco Sedona,*[,a] Mir Masoud Seyyed Fakhrabadi,[a,b] Silvia Carlotto,[a] Elaheh Mohebbi,[a] Francesco De Boni,[a] Stefano Casalini,[a] Maurizio Casarin[a] and Mauro Sambi*[,a,c]

[a]Dipartimento di Scienze Chimiche, Università degli Studi di Padova, Via Marzolo 1, 35131 Padova, Italy
[b]Current address: School of Mechanical Engineering, College of Engineering, University of Tehran, Tehran, Iran.
[c]Consorzio INSTM, Unità di Ricerca di Padova, Padova, Italy

SUPPORTING INFORMATION

1. LEED pattern of the 2,1 GY AgMW and 2,1 GY AgMW structures on Ag(110)

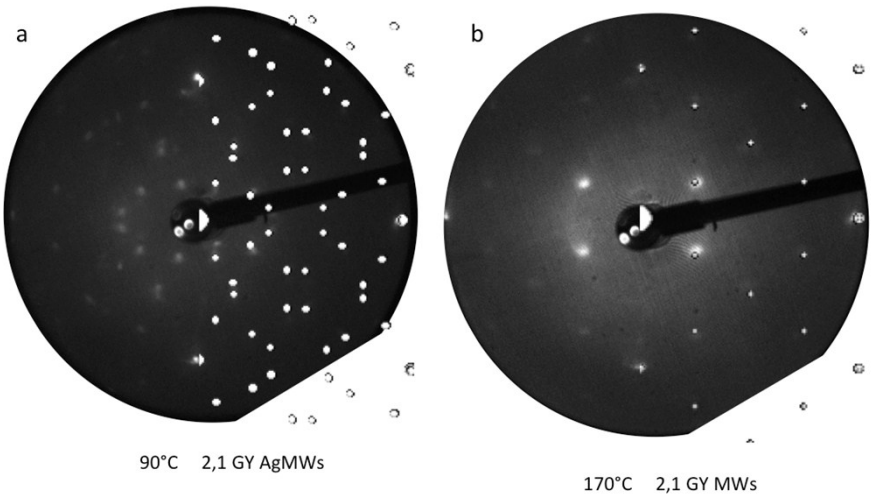

Figure S1. Experimental and superimposed simulated LEED patterns of a) organosilver wires **2,1 GY AgMWs** (48 eV) obtained after deposition of the DBPE precursor on the Ag(110) surface at 90 °C. The simulated LEED pattern corresponds to a commensurate superlattice expressed by the [3±1,-2±3] matrix notation and b) covalent wires **2,1 GY AgMWs** (46 eV) obtained after annealing at 170°C. The simulated LEED pattern corresponds to a commensurate $[3 \pm 1, -1 \pm 1]$ unit cell attributed to Br atoms.

2. DBPE on Ag(111)

XPS analysis

DBPE deposited on Ag(111) held at 90°C and after annealing at 170°C shows XPS spectra very similar to the case when Ag(110) is used as the substrate. In particular, as explained in the main text, it is evident from the analysis of Br 3d peak position and from the C 1s peak fitting that at 90°C DBPE forms an organometallic nanostructure.

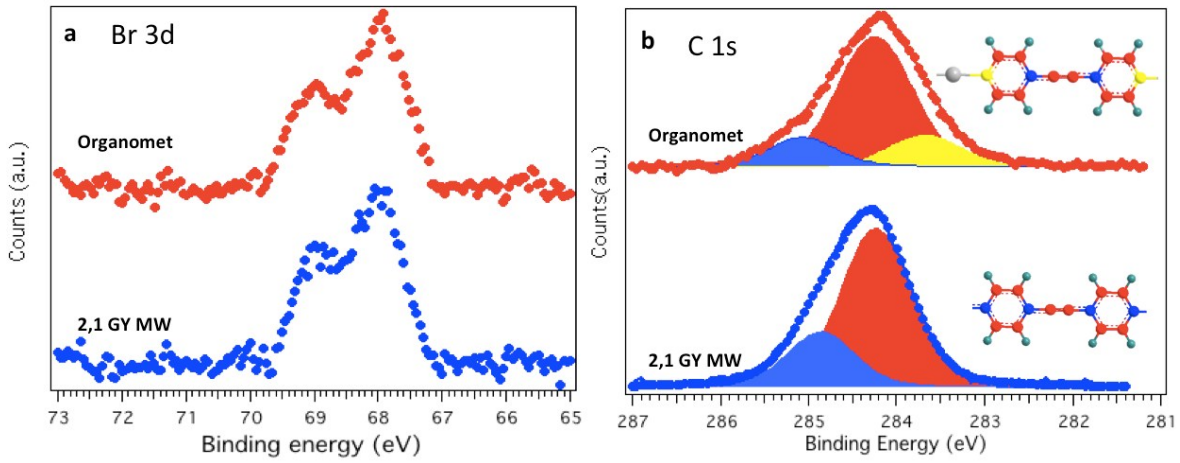

Figure S2: Experimental peaks of (a) Br3d and (b) C1s XPS peaks on Ag(111) of the organosilver structure obtained after annealing at 90 °C and of the **2,1 GY MW** obtained after annealing at 170 °C. Models evidence with different colors the carbon species that contribute to the XPS signal with different components.

LEED pattern of the organosilver **2,1 GY AgMWs** nanostructure

Figure S3. Experimental (40 eV) and superimposed simulated LEED patterns of the DBPE precursor deposited on the Ag(111)

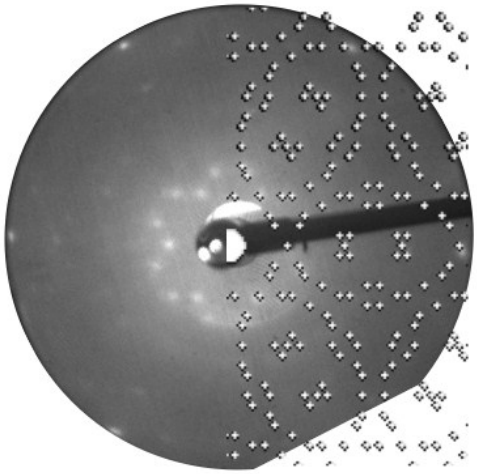

surface kept 90 °C. The simulated LEED pattern corresponds to a commensurate superlattice expressed by the $[5\ 2, 0\ 5]$ matrix notation.

3. Additional computational details

Two different sets of numerical experiments have been performed to reproduce the organosilver **2,1 GY AgMW** and the **2,1 GY MW** ordered phases. In both cases, the Ag(110) surface was modelled by a cell containing five layers, where the top three have been allowed to relax, while the others were kept fixed at their bulk positions. The vacuum region between repeated images along the z direction was large enough to prevent interactions (ca. 16 Å). A bulk optimized lattice parameter of 4.16 Å has been used, which slightly overestimates (1.7%) the experimental value of 4.09 Å [1], but in perfect agreement with other generalized gradient approach calculations.[1] The dimensions of the units cells of the two superstructures are sensitively different: a unit cell 9.75 ×13.79 × 21.84 $Å^3$ including 80 atoms has been employed for the organosilver MW (see Figure S4a), while the dimensions of the **2,1 GY MW** unit cell are 16.63 × 45.83 × 21.84 $Å^3$, which includes 277 atoms (see Figure S4b, where each unit cell contains four debrominated monomers).

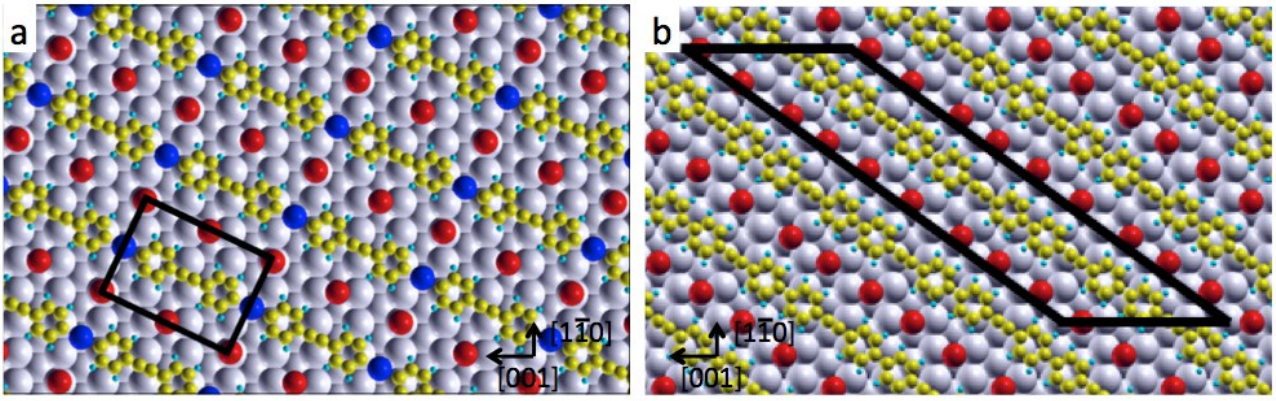

Figure S4. Ball models for supported (a) **2,1 GY AgMW** organosilver phase and (b) **2,1 GY AgMW** phase. Unit cells are outlined by black lines. Color code in models: Br red, C yellow, H light blue, Ag adatoms dark blue, Ag substrate grey.

4. Optimized geometries of the 2,1 GY AgMW and 2,1 GY MW phases with and without dispersion corrections and comparison of experimental and simulated STM images.

2,1 GY AgMW phase calculations

Optimized geometries. In the organosilver phase, major structural variations associated to the presence/absence of dispersion corrections are observed for carbon and hydrogen atoms, while structural parameters of bromine atoms are negligibly perturbed. Indeed, as clearly reported in Figures S5a and S5b, the ligand is strongly curved when dispersion corrections are neglected. The distance of C≡C bonds from the surface is 2.76 Å (3.34 Å) when dispersions are (are not) considered. In general, the inclusion of long-range van der Waals interactions systematically implies a shortening of the distance between the substrate and the organic ligand.

(a) (b)

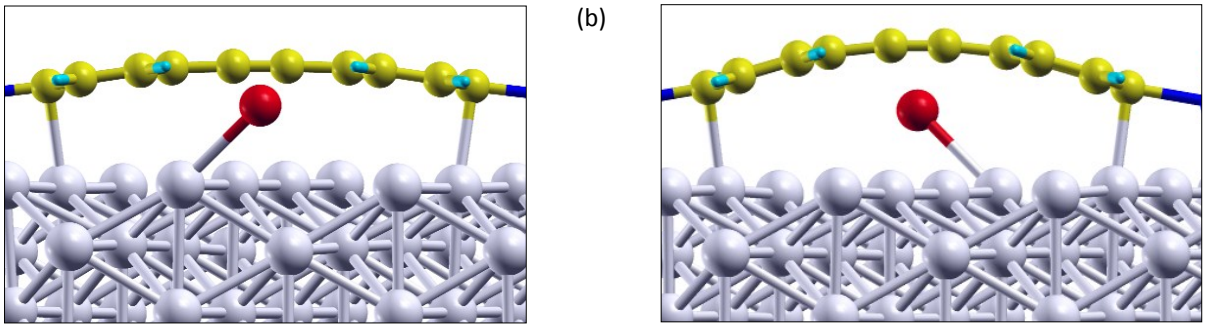

Figure S5. Side view of the organosilver phase ball and stick models (a) with and (b) without dispersion corrections.

Comparison with STM images. Experimental (Figure 6S4a) and simulated (Figures S6b and S6c) STM images of the **2,1 GY AgMW** phase on Ag(110) show a good agreement between theory and experiment with and without dispersion corrections: i) the on-top bromine atoms are brighter than carbon atoms, ii) there is an evident brightness variation for on-top bromine atoms when compared to those occupying long-bridge positions (see the white and grey dots in Figures S6b and S6c, which are the bromine atoms in on-top and long-bridge sites, respectively), and iii) the Ag adatoms are generally brighter than the carbon atoms and their brightness is comparable with that of the on-top bromine atoms.

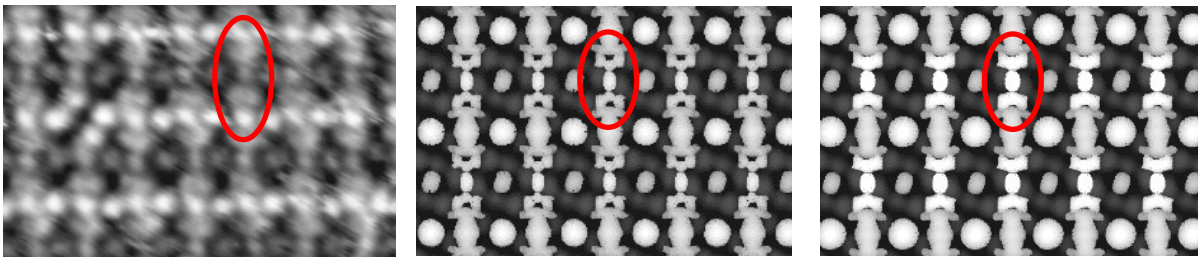

(a) (b) (c)

Figure S6. (a) Experimental and simulated STM images (b) with and (c) without the inclusion of dispersion corrections for **the 2,1 GY AgMW** phase at a bias voltage of V = -0.6 V.

Nevertheless, a careful comparison of experimental and simulated STM images with and without dispersion corrections (see Figures S6b and S6c) demonstrates that the image without corrections overestimates the adsorbate-substrate distance, see the red oval in Figure S6c, which highlights that the brightness of the ethynyl carbon atoms is comparable to that of the on-top bromine atoms. This in not observed in the experimental image (see red oval in Figure S6a). In agreement with the experimental evidence, carbon atoms in the red oval of Figure S6b are less bright than the bromine atoms.

2,1 GY MW phase calculations

Optimized geometries obtained with and without dispersion corrections are displayed in Figure S7. The inspection of Figures S7a and S7b, reveals that, differently from the organosilver case, the inclusion of dispersion corrections has minor effects: the polymer remains in its flat conformation in both cases. The most evident variation is the average distance of the polymer from the surface, which is smaller by ~ 0.5 Å when adopting the dispersion corrections approach.

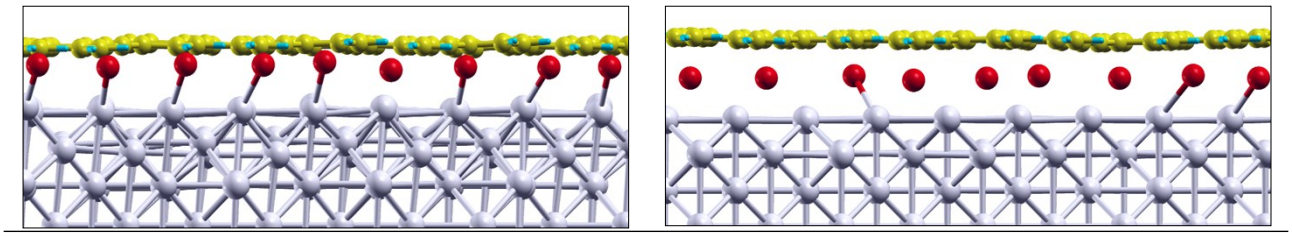

(a) (b)

Figure S7. 2,1 GY MW ball and stick models (a) with and (b) without dispersion corrections.

Comparison with STM images. Also the STM images of the **2,1 GY MW** phase are simulated with and without dispersion corrections. Figure S8 includes the experimental image (Figure S8a), recorded at a bias voltage of -1.0 V, as well as the simulated ones (Figures S8b and S8c). The agreement between experiment and theory is satisfactory in both cases. In particular, simulated images correctly reproduce the following evidences: i) polymer chains are brighter

than bromine atoms, and ii) despite all bromine atoms are in hollow positions, their brightness is variable. The only relevant difference between the two calculations is the overestimated brightness of polymer chains when the dispersion corrections are neglected. The simulation with dispersion corrections included is more similar to the experimental image. Hence, similarly to the **2,1 GY MW** phase, the simulated STM image with dispersions included better fits the experimental ones, even though differences between the two approaches are less evident for the **2,1 GY MW** phase.

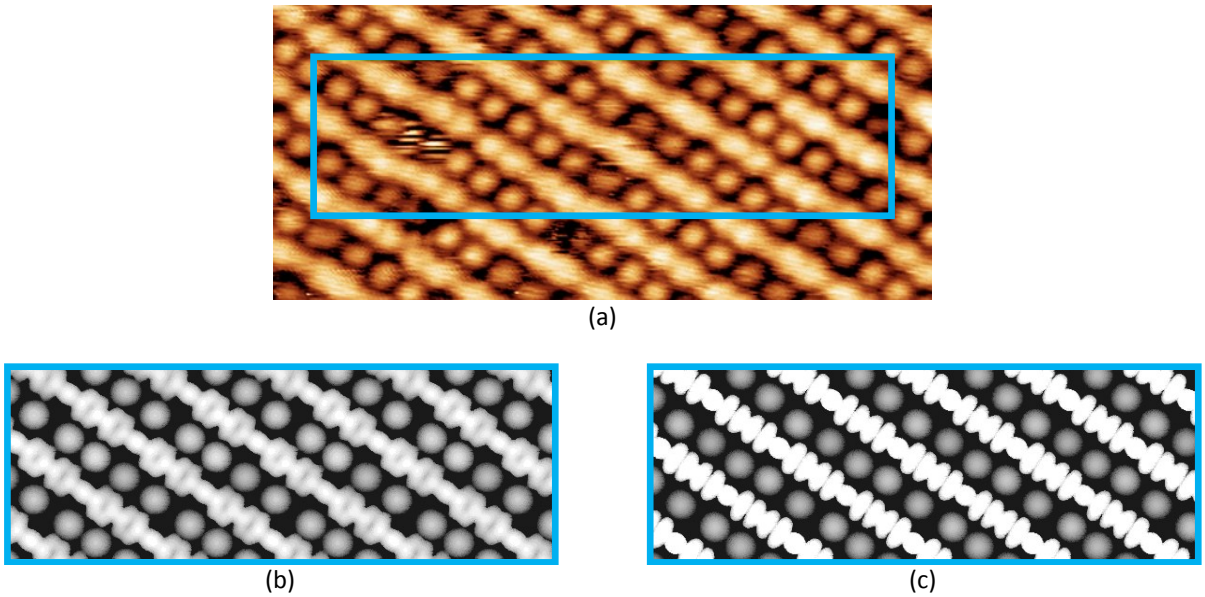

(a) (b) (c)

Figure S8. (a) Experimental and simulated STM images (b) with and (c) without the inclusion of dispersion corrections for the **2,1 GY MW** phase at a bias voltage of V = -1.0 V.

6. Löwdin charge analysis for the optimized geometries with dispersion corrections of the 2,1 GY AgMW and 2,1 GY MW phases.

Further information about the nature of the adsorbate-substrate interactions and the role of the bromine atoms can be obtained by exploiting the Löwdin charge analysis expressed in unit of *e* (e=-1.619x10^{-19} C),[2] which has been limited to the results obtained with the inclusion of dispersion corrections. This analysis was used to determine the charges on different carbon atoms in different systems (see Table S1): i) isolated molecule (ISO), ii) **2,1 GY AgMW** phase (AgMW), iii) **2,1 GY AgMW** phase without the bromine atoms (AgMW*), iv) 2,1 GY MW phase (MW) and v) 2,1 GY MW phase without the bromine atoms (MW*).

The inspection of data collected in Table S1 for the **2,1 GY AgMW** phase reveals that carbon atoms are usually negatively charged with respect to the isolated molecule (ISO); moreover, C_5 are the most negatively charged carbon atoms. C_5 of the AgMW* system have the same charge values, thus stressing the negligible effect of the bromine atoms on the ligand. The carbon atoms (C_1 and C'_1) involved in the triple bond do not undergo significant charge variations and this is supported by the negligible variation of the triple bond length (1.2196 Å *vs* 1.2208 Å, for the isolated and 2,1 GY AgMW supported system, respectively). The charge analysis for the MW and MW* systems reveals i) the same negligible effects of bromine atoms on the charge of carbon atoms and ii) an insignificant charge variation for carbon atoms (C_1 and C'_1) involved in the triple bond with respect to the isolated molecule (bond lengths 1.2196 Å *vs* 1.2348 Å, for the isolated and supported MW system, respectively). The more relevant variations with respected to the isolated molecule are observed for C_5 atoms, which were negatively charged in AgMW (+0.39*e*) and slightly positively charged in MW (-0.04*e*). This difference is due to the different atom involved in the bond with C_5: an Ag adatom in the former and a phenyl ring in the latter case and it is in line with the XPS data.

Table S1. Average total Löwdin charge analysis (in units of *e*) for the C atoms of the isolated molecule and average triple bond lengths (in Å) for low and high temperature 2D patterns. Systems with (*) contain only the molecular systems without the bromine atoms in their optimized geometries. All the charges are reported as derived from the calculations including the dispersion corrections.

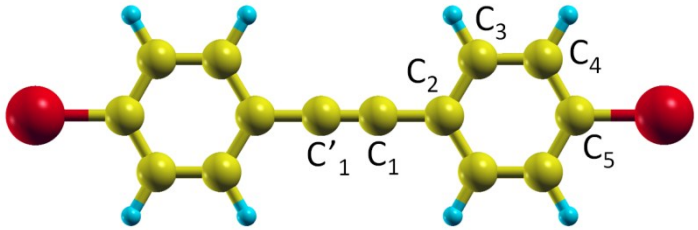

	C_1	C_2	C_3	C_4	C_5	C'_1-C_1
ISO	3.983	3.958	4.085	4.104	4.004	1.2196
AgMW	4.004	3.970	4.113	4.131	4.396	1.2208
AgMW*	4.004	3.968	4.112	4.115	4.393	1.2203
MW	4.000	4.004	4.109	4.122	3.961	1.2348
MW*	4.002	3.973	4.106	4.118	3.965	1.2357

[1] Kokalj, A.; Dal Corso, A.; de Gironcoli, S.; Baroni, S. Adsorption of ethylene on the Ag(001) surface. *Surf. Sci.* **2002**, *507*, 62-68.
[2] Löwdin, P. O. On the non-orthogonality problem connected with the use of atomic wave functions in the theory of molecules and crystals. J. Chem. Phys. 1950, 18, 365–375; (b) Szabo, A.; Ostlund, N. Modern Quantum Chemistry, 1996, Dover.